Liquid-Liquid Phase Transformation in Silicon: Evidence from First-Principles Molecular Dynamics Simulations

N. Jakse[1] and A. Pasturel[1,2]

[1]*Sciences et Ingénierie des Matériaux et Procédés, INP Grenoble, UJF-CNRS, 1130, rue de la Piscine, BP 75, 38402 Saint-Martin d'Hères Cedex, France*

[2]*Laboratoire de Physique et Modélisation des Milieux Condensés, Maison des Magistères, BP 166 CNRS, 38042 Grenoble Cedex 09, France*

(Received 31 July 2007; published 14 November 2007)

We report results of first principles molecular dynamics simulations that confirm early speculations on the presence of liquid-liquid phase transition in undercooled silicon. However, we find that structural and electronic properties of both low-density liquid (LDL) and high-density liquid (HDL) phases are quite different from those obtained by empirical calculations, the difference being more pronounced for the HDL phase. The discrepancy between quantum and classical simulations is attributed to the inability of empirical potentials to describe changes in chemical bonds induced by density and temperature variations.

DOI: 10.1103/PhysRevLett.99.205702 PACS numbers: 64.70.Ja, 61.25.−f, 64.60.My, 71.30.+h

Silicon still remains the material of choice in the semiconductor technology and hence has been the focus of a wealth of fundamental and applied research works [1]. As silicon single crystals are normally formed from the melt, the knowledge of the physical properties in the liquid and undercooled states is then of considerable interest. Beyond the well-known peculiar aspects, such as melting of the crystal into a low-coordinated liquid, accompanied by a semiconductor-to-metal transition as well as a first order liquid-to-amorphous transition [2] in the undercooled region, recent experimental investigations have revealed rich and unusual behaviors of the structural properties as a function of pressure [3] and temperature [4–6]. Undoubtedly, one of the most intriguing features is the possible existence of a transition deeply in the undercooled region from a high-density liquid (HDL) to a low-density liquid (LDL), which was first inferred by Aptekar [7] from thermodynamic considerations. Recent density measurements [8] in the undercooled region, showing an anomalous quadratic behavior, as well as simulation studies [9] are both in favor of its existence.

The coexistence of two forms of liquids in single component substances is one of the most challenging issues in the physics of liquids. For instance, it was directly observed in phosphorus by means of x-ray diffraction experiments [10]. Abrupt and/or anomalous variations of the structural properties as a function of external thermodynamic parameters found in several elemental liquids such as Si, Ge [11], C [12], Cs [13], etc., as well as network-forming liquids such as H_2O, SiO_2, GeO_2 [14], may be indicative of a liquid-liquid phase transition (LLPT) [15,16]. As general interpretation of this phenomenon, Tanaka [17] proposed a model including two competing effects, namely, normal liquid density ordering and bond ordering favoring formation of local structures. Franzese *et al.* [18] have shown that a generic mechanism based on interatomic pair interactions with two characteristic distances is able to generate a LLPT. These approaches suggest that the features of interactions and, in particular, directional bonding play a central role. Indeed, while Sastry and Angell [9] have demonstrated that a LLPT exists for silicon simulated with the Stillinger-Weber (SW) potential [19], Beaucage and Mousseau [20] reported that an arbitrary variation, albeit small, of the parameters of the potential may lead to its disappearance. A similar situation has also been reported in carbon, for which a LLPT was found using an empirical potential [12] while subsequent *ab initio* molecular dynamics simulations [21,22] have found no evidence of it.

As the LLPT for silicon is still inaccessible to experimental investigations because it is thought to be hidden deeply in the undercooled region, the use of predictive first principles simulations is of crucial importance to have a deeper insight regarding this issue, and this is precisely the aim of the present Letter. However, due to cooling rates not higher than 2×10^{10} K/s to obtain the LLPT for silicon as discussed below, it would be prohibitively expensive to study the LLPT using only such an approach. We therefore use a mixed approach by combining efficiently classical and first principles molecular dynamics. The high density and the low density liquids near the transition are generated in a first stage from classical molecular dynamics simulations (MD). For the latter, the SW potential is the natural candidate since it displays an LLPT [9]. Starting from configurations obtained on both sides of the LLPT, our first principles MD simulations evidence for the first time an HDL as well as an LDL state, regardless of a specific empirical interaction model.

We follow the protocol defined by Sastry and Angell [9] to analyze the behavior of silicon in the undercooled regime. Figure 1 visualizes the evolution of the density and the enthalpy (inset) during the simulation procedure, which lasted 36.3 ns, i.e., 2.41×10^7 time steps. Starting from a well equilibrated liquid at $T = 1750$ K near the

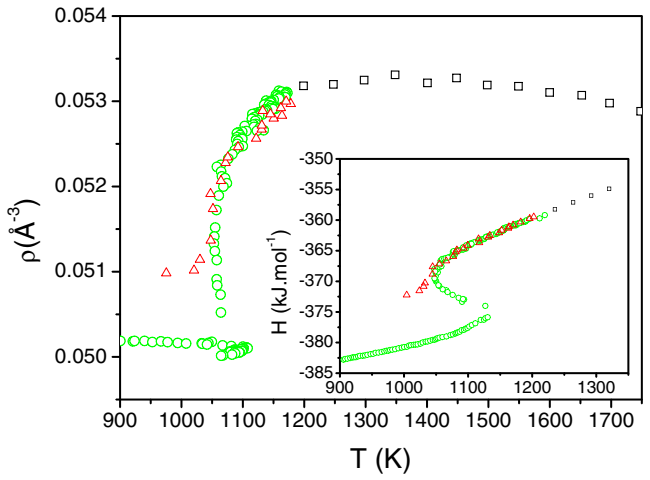

FIG. 1 (color online). Number density as a function of temperature: the squares and circles represent, respectively, the *NPT* and *NPH* molecular dynamics simulations with the Stillinger-Weber potential. Triangles represent MD simulations in the *NPH* ensemble with a higher quenching rate (see text). The inset shows the enthalpy as a function of temperature (same captions as the main panel).

melting point, simulations in the *NPT* ensemble with $N = 512$ silicon atoms are used, and the system is cooled down in the undercooled regime at $T = 1200$ K above the expected liquid-liquid transition ($T \sim 1060$ K) [9] with a quenching rate of 10^{11} K/s. This is done by changing the reference temperature of the thermostat using a ramp [23]. At $T = 1200$ K, the thermostat is then switched off, and the simulation is continued in the *NPH* ensemble to capture the phase transition. The system is cooled further by decreasing the enthalpy of the system periodically with a mean quenching rate of 2×10^{10} K/s. The enthalpy decreases monotonically with temperature down to $T = 1050$ K. A further decrease of the enthalpy induces a rise of the temperature, which is a clear signature of the production of a latent heat of transformation in the system identified as a LLPT by Sastry and Angell [9]. When the enthalpy is further reduced, the temperature drops again, and an amorphous state is obtained. It should be noted that increasing of the mean quenching rate, only up to 4×10^{10} K/s, leads to a bypassing of the LLPT and to the formation of an amorphous state, as shown in Fig. 1. This emphasizes that the LLPT found at about $T = 1050$ K can be attained by MD simulations at the condition that the system is brought in its vicinity with an appropriate cooling rate.

Having obtained equilibrium configurations in the HDL and LDL states by classical MD, namely, at $T = 1050$ K and $T = 1070$ K with respective densities $\rho = 0.0523$ and 0.050 Å^3, we address the important question on the stability of these two liquid phases, independently of the interactions used to describe them. For this purpose, first principles molecular dynamics (FPMD) simulations are carried out in the canonical ensemble (*NVT*) with $N = 512$ silicon atoms, taking the above-mentioned configurations as initial ones. The electronic structure calculations are performed within the density functional theory (DFT) with the generalized gradient approximation (GGA) [24]. We use the most recent version of the Vienna *ab initio* simulation package (VASP) [25] in which the interaction between the ions and electrons is described by the projector augmented-wave (PAW) method, as implemented by Kresse and Joubert [26]. In the PAW potential, $2s$ and $2p$ orbitals are treated as valence orbitals with a plane wave cutoff of 245 eV. Only the Γ-point is used to sample the Brillouin zone. For the sake of comparison, an additional run has been done at $T = 1750$ K, in the liquid above the melting point. Using a time step of 1.5 fs as for the classical simulations, the time span of the FPMD simulations is 25 ps at $T = 1050$ K, 42 ps at $T = 1070$ K, and 20 ps in the stable liquid [27]. Because of the switching of the forces at the initial time from the SW potential to the interactions calculated from first principles, an evolution of the properties towards new equilibrium values are seen. Therefore, by following static properties such as the coordination number and bond-angle distribution during the first part of the runs, we have found that this evolution has ended roughly after 10 ps for both states. Therefore, the bias that could have been induced by the SW potential in the initial configurations is cancelled out, and we will see that this evolution is mainly due to the fact that the SW potential significantly underestimates the changes in the local structure induced by density and temperature variations. Finally, the properties of interest were calculated from the remaining part of simulations. It is worth mentioning that the enthalpies for the HDL and LDL obtained from the *ab initio* calculations are respectively -468 and -474 kJ/mol. The SW potential overestimates by 20% these values which can be attributed to its empirical nature. Nevertheless, the key quantity which is the enthalpy difference between the HDL and LDL is similar for both calculations, namely -5.5 kJ/mol for the SW model and -6 kJ/mol for *ab intio* calculations.

We consider first the mean-square displacement $R^2(t)$ in order to check whether the phases simulated by FPMD at $T = 1050$ K and $T = 1070$ K are still liquids and to distinguish them from their amorphous counterparts. Figure 2 shows the evolution of the function $R^2(t)/6t$ with respect to time: after a marked cage effect, it becomes a non zero constant at long times, indicating that $R^2(t)$ has a linear behavior for both temperatures. This diffusive regime is expected for liquids and confirms that the two states at $T = 1050$ K and $T = 1070$ K are in a high-density liquid and a low-density liquid, respectively, during the time of the simulations. The corresponding self-diffusion coefficients D are $D = 9.2 \times 10^{-6}$ cm^2/s in the HDL phase and $D = 4.8 \times 10^{-7}$ cm^2/s in the LDL phase, showing that, crossing the transition from the HDL to the LDL, the diffusivity

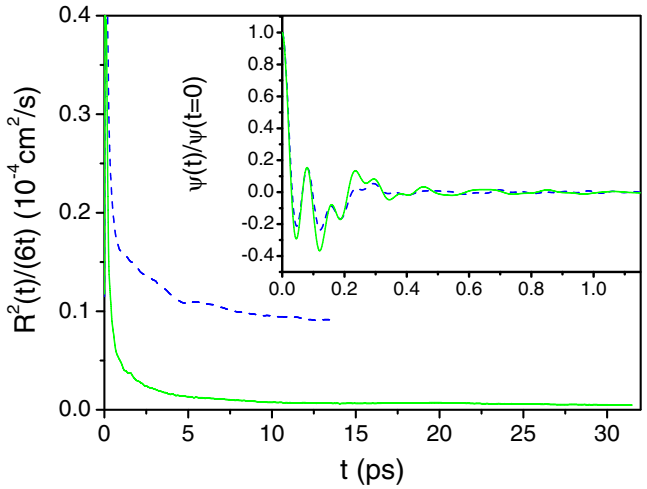

FIG. 2 (color online). Mean-square displacement divided by time for the high-density liquid at $T = 1050$ K (dashed line) and low-density liquid at $T = 1070$ K (solid line) obtained from the first principle molecular dynamics simulations. The inset displays the corresponding velocity autocorrelation functions.

decreases roughly by an order of magnitude but remains significant. The same values of D are obtained from the corresponding velocity autocorrelation functions (inset). It should be noted that, while the value in the HDL is close to that obtained from the SW potential, it is higher by an order of magnitude in the LDL [9].

The structural changes from the stable liquid to the HDL, and then to the LDL can be seen in Fig. 3. Above the melting point, the pair-correlation function, $g(r)$, is in good agreement with our experimental data [5] (not shown). Upon undercooling in the HDL state, the first peak of the pair-correlation function sharpens, and the amplitude of the subsequent oscillations enhances substantially. Going from the HDL to the LDL, an evolution of $g(r)$ is seen essentially at the level of the second peak. For each state, the coordination number is calculated by counting the number of atoms in the first coordination shell whose radius corresponds to the first minimum of $g(r)$. It takes the value $N_C = 6.4 \pm 0.04$ at $T = 1750$ K, close to those found in several recent experiments [4–6] and the value of 6.22 ± 0.05 obtained from classical simulations. The coordination number reduces to $N_C = 4.36 \pm 0.04$ at $T = 1050$ K for the HDL while in the LDL, we have found $N_C = 4.08 \pm 0.04$, which is slightly lower, but distinct from the value in the HDL. The distribution of the coordination number around individual atoms shown in Fig. 3(b) reveals that a large majority of the atoms are four-coordinated in the LDL, while in the HDL, the number of atoms with coordination 5 and 6 is still important. Let us mention that the values obtained from classical simulations are 5.15 and 4.67 for HDL and LDL, respectively. These values are larger than those obtained from *ab initio* calculations, indicating the difficulty of empirical potentials to describe the changes in chemical bonds induced by density

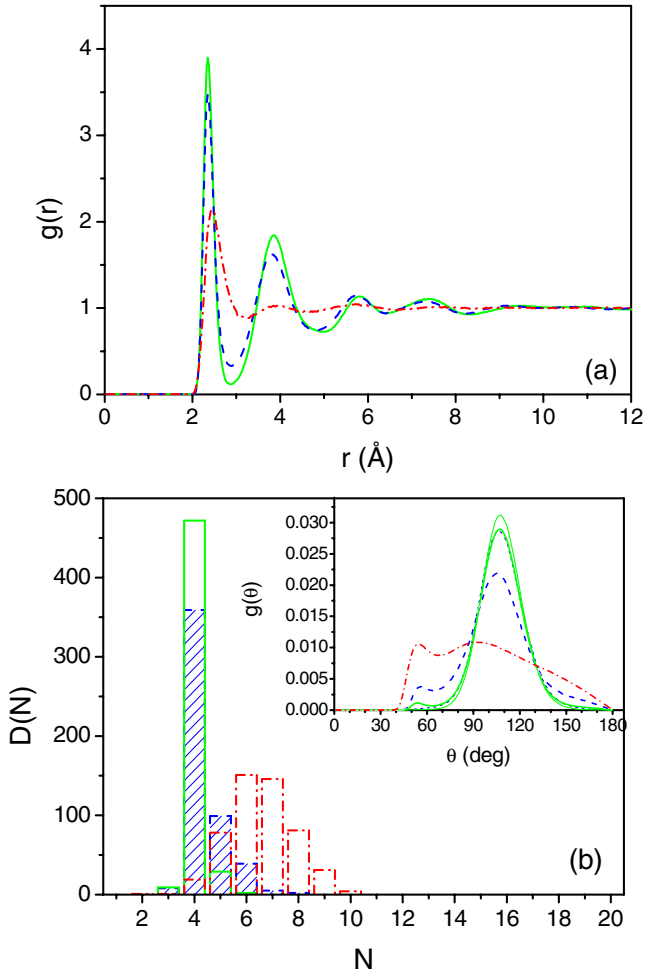

FIG. 3 (color online). (a) Pair-correlation function for $T = 1750$ K above the melting point (dash-dotted line), the high-density liquid at $T = 1050$ K (dashed line) and low-density liquid at $T = 1070$ K (solid line) obtained from the first principle molecular dynamics simulations. (b) Distribution of the coordination numbers around individual atoms for $T = 1750$ K above the melting point (dash-dotted line), the high-density liquid at $T = 1050$ K (dashed line and hatched surface), and low-density liquid at $T = 1070$ K (solid line). The inset shows the bond-angle distribution for the three temperatures [captions are the same as panel (a)]. The corresponding thin lines are the distributions around four-coordinated atoms.

and temperature variations. Using first-principles MD simulations, Morishita [28] found also a drastic increase of the tetrahedrality around 1200 K. However, his coordination number at 1100 K is greater than our values. Such a discrepancy is due to the use of a quenching rate higher nearly by 2 orders of magnitude than that used in the present work. As discussed above, increasing the quenching rate may lead to an incorrect description of thermodynamic properties of liquid silicon upon undercooling. The bond-angle distribution in the inset of Fig. 3(b) is illuminating regarding the mechanism of the LLPT for silicon: It displays a strong maximum at 109°, showing the establish-

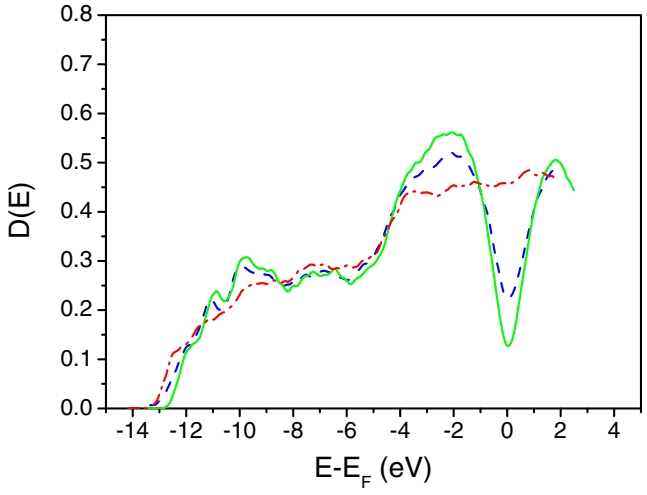

FIG. 4 (color online). Electronic density of states for $T = 1750$ K above the melting point (dash-dotted line), the high-density liquid at $T = 1050$ K (dashed line), and low-density liquid at $T = 1070$ K (solid line) obtained within the DFT.

ment of a local tetrahedral arrangement in the LDL. In the HDL atoms contributing to the bond-angle distribution at 55° are typically interstitial atoms (fifth and sixth atom in the first coordination shell) which are pushed back in the second coordination shell upon crossing the transition, in agreement with the evolution of the second peak of the pair-correlation function. This demonstrates that locally favored tetrahedral structures play an important role here [17].

This tetrahedral arrangement should reflect in the electronic properties. We have therefore determined the electronic density of states (DOS) for the HDL and the LDL as well as for the stable liquid. Configurations have been extracted from the runs for the electronic structure calculations, and we have used eight Monkhorst-Pack points in sampling the Brillouin Zone of the 512-atom supercells. Figure 4 shows the curves of the DOS obtained for the three liquids. In the stable liquid, the DOS does not display a pseudogap at the Fermi energy indicating that the system exhibits a metallic character. A pseudogap is formed in the HDL and enhances in the LDL which is a consequence of the formation of local tetrahedral structures due to a more covalent nature of atomic bonding, as pointed out by Ashwin *et al.* [29]. However, in the HDL, the authors did not find a pseudogap in the DOS. Again, such a discrepancy can be attributed to the empirical nature of the SW potential, yielding atomic configurations with a coordination number over 5 in the HDL and the metal-to-semimetal transition accompanying the LLPT as observed by Ashwin *et al.* [29] must be related to this overcoordination.

To summarize, we have used a combined classical and first principles molecular dynamics simulation scheme to study the deep undercooled region of silicon near the liquid-liquid transition around $T = 1050$ K. We have shown the existence of a high-density as well as a low-density liquid, regardless of a specific empirical interaction model, which is in favor of a liquid-liquid phase transition. Our findings further reveal the enhancement of tetrahedral local structures in going from the HDL to the LDL, and do not support the metal-to-semimetal transition accompanying the LLPT as observed in classical simulations [29].

We acknowledge the CINES and IDRIS under Project No. INP2227/72914 as well as PHYNUM-CIMENT for computational resources.

[1] W. C. O'Mara, R. B. Herring, and L. P. Hunt, *Handbook of Semiconductor Silicon Technology* (*William Andrew Publishing*, Noyes, 1990).
[2] E. P. Donovan *et al.*, J. Appl. Phys. **57**, 1795 (1985).
[3] N. Funamori and K. Tsuji, Phys. Rev. Lett. **88**, 255508 (2002).
[4] H. Kimura *et al.*, Appl. Phys. Lett. **78**, 604 (2001).
[5] N. Jakse *et al.*, Appl. Phys. Lett. **83**, 4734 (2003).
[6] T. H. Kim *et al.*, Phys. Rev. Lett. **95**, 085501 (2005).
[7] L. I. Aptekar, Sov. Phys. Dokl. **24**, 993 (1979).
[8] Z. Zhou, S. Mukherjee, and W. K. Rhim, J. Cryst. Growth **257**, 350 (2003).
[9] S. Sastry and C. A. Angell, Nat. Mater. **2**, 739 (2003).
[10] Y. Katayama *et al.*, Nature (London) **403**, 170 (2000).
[11] K. Tsuji *et al.*, J. Phys. Condens. Matter **16**, S989 (2004), and references therein.
[12] J. H. Glosli and F. H. Ree, Phys. Rev. Lett. **82**, 4659 (1999), and references therein.
[13] S. Falconi *et al.*, Phys. Rev. Lett. **94**, 125507 (2005); Phys. Rev. B **73**, 184204 (2006).
[14] C. J. Roberts, A. Z. Panagiotopoulos, and P. G. Debenedetti, Phys. Rev. Lett. **77**, 4386 (1996).
[15] C. A. Angell, Science **267**, 1924 (1995); P. H. Poole *et al.*, Science **275**, 322 (1997).
[16] H. Tanaka, Phys. Rev. E **62**, 6968 (2000).
[17] H. Tanaka, Phys. Rev. B **66**, 064202 (2002).
[18] G. Franzese *et al.*, Nature (London) **409**, 692 (2001); G. Franzese, M. I. Marques, and H. E. Stanley, Phys. Rev. E **67**, 011103 (2003); A. Skibinski *et al.*, Phys. Rev. E **69**, 061206 (2004).
[19] F. H. Stillinger and T. A. Weber, Phys. Rev. B **31**, 5262 (1985).
[20] P. Beaucage and N. Mousseau, J. Phys. Condens. Matter **17**, 2269 (2005).
[21] C. J. Wu *et al.*, Phys. Rev. Lett. **89**, 135701 (2002).
[22] X. Wang, S. Scandolo, and R. Car, Phys. Rev. Lett. **95**, 185701 (2005).
[23] M. P. Allen and D. J. Tildesley, *Computer Simulation of Liquids* (Clarendon Press, Oxford, 1989).
[24] Y. Wang and J. P. Perdew, Phys. Rev. B **44**, 13298 (1991).
[25] G. Kresse and J. Furthmüller, Comput. Mater. Sci. **6**, 15 (1996); Phys. Rev. B **54**, 11169 (1996).
[26] G. Kresse and D. Joubert, Phys. Rev. B **59**, 1758 (1999).
[27] S. Nosé, J. Chem. Phys. **81**, 511 (1984).
[28] T. Morishita, Phys. Rev. Lett. **97**, 165502 (2006).
[29] S. S. Ashwin, U. V. Waghmare, and S. Sastry, Phys. Rev. Lett. **92**, 175701 (2004).